IJBPAS, April, 2023, 12(4): 1462-1476

ISSN: 2277–4998

International Journal of Biology, Pharmacy and Allied Sciences (IJBPAS)

'A Bridge Between Laboratory and Reader'

www.ijbpas.com

EFFICIENCY OF TIN OXIDE (SnO_2) AS CORROSION INHIBITORS FOR ALUMINIUM

MUGILA P AND SILAMBARASAN J*

Department of chemistry, Theivanai Ammal College for Women (A), Villupuram, Tamil Nadu, India.

***Corresponding Author: Dr. J. Silambarasan: E Mail: j.silambarasan@gmail.com**

Received 8th May 2022; Revised 16th June 2022; Accepted 27th Aug. 2022; Available online 1st April 2023

https://doi.org/10.31032/IJBPAS/2023/12.4.7010

ABSTRACT

Herein, we synthesized tin oxide nanoparticles using sol-gel method. XRD and SEM were used for characterizing metal oxide nanoparticles. The corrosion resistance behaviour of the SnO_2 nanorods has been studied by using it as inhibitor for corrosion of Aluminium in 5% HCl by weight loss, Tafel polarization and electrochemical impedance spectroscopy methods. From corrosion studies it can be concluded that, the SnO_2 nanorods can be used as a potential inhibitor for corrosion of aluminium in 5% HCl.

Keywords: Aluminium, Tin Oxide nanorods, SEM, XRD, Impedance, Corrosion

INTRODUCTION

Corrosion is the deterioration of materials for the reason that reaction with its environment. It will leads to vast loses in a variety of industrial systems and household processes by causing significant degradation, catastrophic failure, and major accidents, which lead to huge losses. These disadvantages are contributing directly or indirectly to the country's economic losses. Therefore, many kinds of research on corrosion are ahead dominant position from added than a century **[1, 2]**. The kinetics of corrosion be influenced by the nature of material and the environment. Various methods have been proposed so far to restrict corrosion in a different environment. However, the selection of preventive process depends upon the various factors such as process cost, process performance, and corrosion effects **[3]**.

The corrosion protective coatings are widely utilized in this regard owing to availability of a variety of coating materials and processes for different environmental conditions, and applications. The main objective of the corrosion-resistant coatings is to protect metals and alloys, making an effective wall against corrosive species surviving in different environments **[4]**, including water, hot corrosive fluids, soils, ultraviolet radiation, and air pollution. Furthermore, coatings on structures submerged in water or suppressed under soil surface humidity and microorganisms **[5, 6]**. The long contact to corrosive environment results in breaking of the coating barrier, thereby allowing the ingress of aggressive ions. Once the coating is broken, it cannot stop further ingress of the corrosive ions, and an unreliable zone is formed, which starts propagating and leads to total failure of coating **[7]**. These are the major worries, particularly when dealing with organic coatings. Therefore, an active protection system, which slows down corrosion process or self-heals the defect, is required for appropriate component life. For the improvement of corrosion resistance, one or more of the following ways are utilized to protect the metal substrate such as the use of corrosion inhibitors or a coating that can provide a resistant barrier to water and corrosive species **[8, 9]**.

Coatings are deposited on the surface of substrate, or the NPs are incorporated into them to acquire productive results. These techniques not only perform well as far as corrosion protection is concerned but also optimize the other properties of the coatings. Moreover, the corrosion inhibitors are introduced into coatings to improve the performance and hinder the ingress of corrosive ions to the defective sites **[10, 11]**. Usually, the inhibitors used have hysterical healing of defects, which cause blistering in coatings **[12]**. The inhibitors used have hysterical healing of defects, which cause blistering in coatings **[13]**. For controlled healing of defects, several strategies, i.e., encapsulation of corrosion inhibitors **[14]**, layer-by-layer oxide films **[15]**, nanocontainers **[16]**, and metal/metal oxide NPs **[17]** are suggested

To date, there has been significant research **[18]** to improve the performance of different metallic materials. Aluminium and its alloys **[19]** have been applied in many different kinds of fields. However, the poor corrosion resistance caused by the active chemical properties of aluminium and its alloys has greatly influenced their operation life and application. Therefore, current

research is focused on improving the corrosion resistance of aluminium and its alloys, such as the preparation of superhydrophobic surface **[20]**, metallic oxide film surface **[21]**, and alloying surface **[22]** and so on.

In this study, Ultra fine SnO_2 nanoparticles is successfully synthesized to improve the corrosion of Aluminium in an acidic environment. Evaluate the inhibition effect of as synthesized SnO_2 for aluminium corrosion using weight loss, Tafel polarization and electrochemical impedance spectroscopy techniques.

2. EXPERIMENTAL PROCEDURE

Materials

Tin chloride ($SnCl_2$, Merck 99 %) as starting material, trichloroethylene as surfactant, absolute HCl as a solvent, ortho phosphoric acid as precipitator were used to prepare tin oxide nanoparticles. All the solutions were prepared using double distilled water.

Synthesis of SnO_2 powder

To 0.5 M $SnCl_2$, 10 ml of HCl was added. The mixture was then heated and to the clear solution, 20 ml of H_3PO_4 was added drop by drop. The solution was continuously stirred for 3 hrs at room temperature. After 3 hrs the product was formed completely and the solution was decanted and the product was washed with water and ethanol. Then it was filtered and dried in hot air oven (or) in muffle furnace and the yield was noted.

Corrosion studies

The inhibitive effect of the as synthesised SnO_2 was studied by using it as corrosion inhibitor for corrosion of aluminium in 5% HCl by weight loss mothed, potentiodynamic polarization and electrochemical impedance, spectroscopy techniques.

Weight loss method

Preweighed aluminium specimens were immersed in 5% HCl at various immersion times ranging from 1800-9000 sec at various temperatures from 303K-323K. The effect of inhibitors on corrosion of aluminium specimen was studied by immersing the specimens in 5% HCl containing various concentration ranging from 0.08%-0.2% of the inhibitors at various immersion times and temperatures.

Aluminium plates were hanged above the corrosion medium taken in a beaker in such a way that, the solution is up to 5cm from the bottom of the plate. After the duration of immersion time, each specimen was removed from the solution, washed thoroughly using distilled water and dried. The samples were finally weighed, the difference in weights was noted and the

corrosion rates inhibition efficiency and surface coverage were calculated.

Measurement of corrosion rate

The rate of corrosion was evaluated using the equation

$$K = \frac{(83.4 \times 1000 \times W)}{(A \times D \times t)}$$

where, A = area of the specimen immersed

W = difference in weight after and before corrosion

D = density of metal

t = time

The rate is expressed in mills per year.

Determination of inhibition efficiency

The percentage of inhibition efficiency (IE) was calculated by using the equation

$$I.E(\%) = [1-(k_{in} / k_{unin})] \times 100$$

where, k_{in} and k_{unin} are the corrosion rates of aluminium in the presence and absence of inhibitor respectively.

Determination of surface coverage

Surface coverage values were calculated from the equation

$$\text{Surface coverage } \theta = [1-(k_{in} / k_{unin})]$$

Potentiodynamic TAFEL polarization studies

Potentiodynamic polarization studies were carried out at room temperature in 5% HCl using the Electrochemical Workstation model 760 supplied by CH Instruments. The potentiodynamic polarization studies were carried out in three compartment cell in which platinum electrode was used as counter electrode Calomel electrode as reference electrode and aluminium as working electrode. The reference electrode was connected with test solution through a salt bridge. After 30 minutes, I_R - compensation was done and potentiodynamic polarization studies were carried out.

The Tafel polarization studies were carried out from the cathodic potential of -900 mV (vs. SCE) to the anodic potential value of -60 mV (vs. SCE) at a scan rate of 10 mV/s. This scan rate was selected based on the differential trial experiments to get reproducible results representing some steady state conditions for the electrodic reaction. Within 100 mV from the OCP, tangents were drawn and the Tafel slopes were estimated. E vs log i curves were then recorded. The Tafel slopes b_a and b_c were determined from the slopes of the anodic and cathodic slopes of the Tafel plots and the intercept gives i. From the i value, the rate of corrosion k in mpy was calculated.

$$k = i \times 1.288 \times 10^{-3} \text{ mpy}$$

Electrochemical impedence spectroscopic studies

The inhibitive effect of nanocrystalline SnO_2 powder was further confirmed by electrochemical impedence

spectroscopy. Impedence measurements were performed in 5% HCl using impedence analyzer in the frequency range of 10 MHz to 100 KHz with an AC modulation at amplitude of 5 mV. The cell set up used was exactly same as that of Tafel polarization studies.

Nyquist impedance plots were recorded for Al samples in 5% HCl containing various concentration of SnO_2 as inhibitors from 0.08% to 0.2% for various immersion periods from ½ hr to 2 ½ hr. From the semicircules of the Nyquist plots, the Rs, Rp and (c) values were determined.

Adsorption isotherm studies

Langmuir adsorption isotherm was obtained by plotting C/θ vs C where C is the concentration of inhibitor and θ is the surface coverage. Freundlich adsorption isotherm was obtained by plotting logC Vs logθ.

3. RESULTS AND DISCUSSION

XRD analysis

The surface nanostructure and texture of the synthesized SnO_2 nanorods were analysed by XRD. **Figure 1** shows the XRD pattern of synthesized SnO_2 nanorods. Sharp peaks are observed which indicate the powder is made up of nanocrystals. The XRD inferred that the SnO_2 nanorods are having only one phase with different crystal sizes and planes.

The results indicate that, the product comprises of pure phase and there is no impurity peaks. The sharp peaks indicate that the products were well crystallised. The diffraction peaks were in good agreement with those given in the standard data (PCPDF, 79-0207) for SnO_2 and showed a good crystallinity. This means that, as the prepared materials were crystallized in a hexagonal rutile structure of SnO_2 with the mean crystallite size, d is in inverse proportion to the full width at half maximum β(d=0.89 λ /(βcosθ), indicating that, the initial grain size to decrease.

The mean crystallite size d, was measured from the XRD (D.MAX-YB, RIGAKU) peaks at a scanning rate of 5º/min based on Scherrer's equation

$$d = \frac{0.9\lambda}{\beta\cos\theta'}$$

where λ is the wavelength of the X-ray, θ is the diffraction angle, and β is the full width at half maximum. The size of the SnO_2 crystallites ranged from 4 to 173 nm and the average crystallite size is 74 nm.

Surface morphology

Figure 2 shows the surface morphologies of the synthesized SnO_2 powder. From the SEM images, it can be

observed that, the synthesized SnO_2 particles are having rod shape, with varying diameters ranging from 400-800 nm. It can be seen that, some of the rod shaped particles are agglomerated and appear as platelets or sheets. Form the size, shape and diameters of the particles, one can infer that, the synthesized SnO_2 powder is the agglomeration of nanorods. The nanostructure and size can be further confirmed by XRD studies.

Deformation area near the crystal grain boundary is seen. May be it was caused by squeezing between crystals. From **Figure 2**, it can be seen that, the crystal lattice was distorted by the grain squeeze which reveals that, deformation always occurs around crystalline exterior.

Corrosion studies

Weight loss measurements

Effect of immersion time

The corrosion of aluminium specimens in 5% HCl at various temperatures for various times was studied by weight loss method and the corrosion rates were evaluated. **Figure 3** shows the effect of immersion time on the rate of corrosion of aluminium in 5% HCl at various temperatures ranging from 303 K-323K.

From the **Figure 3**, it is inferred that, as immersion time increases, the rate of corrosion increases at all temperatures. This is because, as the immersion time increases, the substrate and the attacking molecules of the medium are contacting for longer time and hence the dissolution of metal taking place at a faster rate.

In order to inhibit the corrosion rate of aluminium and to test the inhibiting effect of synthesized nanocrystalline SnO_2, aluminium specimens were immersed in 5% HCl containing various concentrations of SnO_2 at various temperatures and durations. The corrosion rate, percentage of inhibition efficiency and surface coverage were evaluated. **Figure 4** show the effect of immersion time on rate of corrosion of aluminium in 5% HCl containing various concentrations of the inhibitor. From the figs, it can be inferred that, as the immersion time and temperature increases the rate of the corrosion also increases.

Figure 5 show the effect of immersion time on surface coverage of the inhibitor on aluminium surface at various temperatures for various concentrations. From the **Figures 5** it can be sent that the surface coverage increases with increase of immersion time. The reason is same as that of inhibition efficiency.

Also, it can be observed that, as in the case of without inhibitor, corrosion rate

increases with increase of temperatures. But the corrosion rate decreases with addition of inhibitors and it decreases with increasing concentration of inhibitors. This is because, as the concentration of inhibitor on aluminium surface increases, the extent of adsorption of inhibitor increases and formation of thin protective film over the metal surface also increases.

From the **Figures 5**, it is clearly seen found that, the maximum percentage of inhibition efficiency and surface coverage are obtained for 0.01gpl inhibitor. The reason for the increase in inhibition efficiency and surface coverage with increase in concentration of inhibitor is due to the masking of aluminium substrate by the inhibitor which inhibits the attack of corroding medium on the aluminium surface. As the concentration of inhibitor increases, more number of inhibitor molecules adsorbed on the surface and hence gave strong protection to the metal by forming a protective layer. So surface coverage and inhibition efficiency increase with increase in concentration of inhibitor.

Effect of temperature

From the **Figures 5**, it can be seen that, as the temperature of the corroding medium both in the presence and absence of inhibitor is increased, the rate of corrosion was found to increase and the % of inhibition efficiency and surface coverage were decreased. As the temperature of the system increases, two effects were taking place. One is, the adsorbed molecules undergo dissociation and hence the protective film gets damaged. Second one is, at higher temperatures, desorption of inhibitor is taking place and the protective layer on aluminium surface was removed so there is an increase in attack of corrosion solution on aluminium at higher temperatures. Hence the rate of corrosion increases and inhibition efficiency and surface coverage decreases with increase of temperature.

Adsorption isotherm

In order to know the type of adsorption of inhibitor on aluminium surface, the concentration of the inhibitor and surface coverage values were fitted with Langmuir and Freundlich adsorption isotherm plots. **Figure 6** show the Langmuir adsorption plots for the adsorption of inhibitor on aluminium substrates and **Figure 7** show the Freundlich adsorption plots for the same. From the straight lines obtained from the both of the plots, the adsorption of inhibitors followed both Langmuir and Freundulich adsorption isotherms.

Tafel polarization studies

The electrochemical behaviour of corroded aluminium was studied by Tafel polarization studies. **Figure 8** shows the comparative Tafel plots for aluminium in 5% HCl without and with various concentration of inhibitor. The parameters E_{corr}, I_{corr}, R_{corr} were calculated and presented in **Table 1**. From the table and figure, it was observed that the I values decreases and E value increases for inhibitor compared to that of the blank solution, which indicates the inhibitor reduces the rate of corrosion of aluminium. Lowest corrosion rate value was obtained for Aluminium immersed in 5% HCl containing 0.04gpl inhibitor.

AC Impedance spectroscopic studies

The corrosion of aluminium was also studied by electrochemical impedance spectroscopy. **Figure 9** show the comparative Nyquist impedance diagrams for corrosion of aluminium for the blank and various concentration of inhibitor. The impedance spectrum of each specimen is characterized by well-defined curves. From the figure, it is inferred that, Al sheet immersed in 5% HCl containing inhibitor has higher impedance which conformed the rate of corrosion is inhibited by the SnO_2 and best inhibition is obtained for aluminium immersed in 5% HCl containing 0.04gpl inhibitor. This is due to the formation of a layer by adsorption of the inhibitors on metal surface which prevents the attack of the corrosion solution and hence inhibit the rate of corrosion. The R_s, R_p and C values were evaluated from the Nyguist diagrams. From the **Table 1** it can be seen that R_p values increased and C values decreased with increase of concentration of inhibitor. This is well explained the inhibiting effect of the synthesized SnO_2 powder.

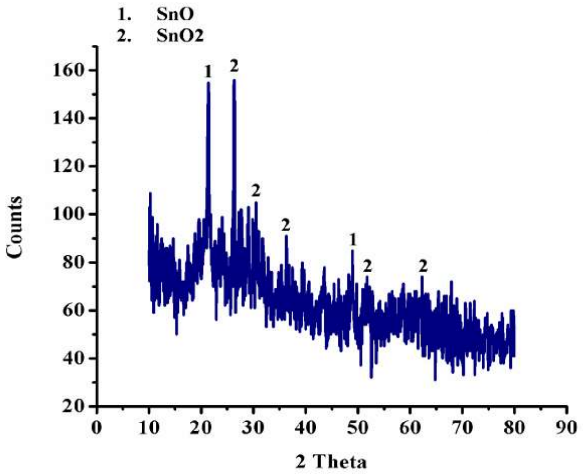

Figure 1: X-ray diffraction pattern of the SnO_2

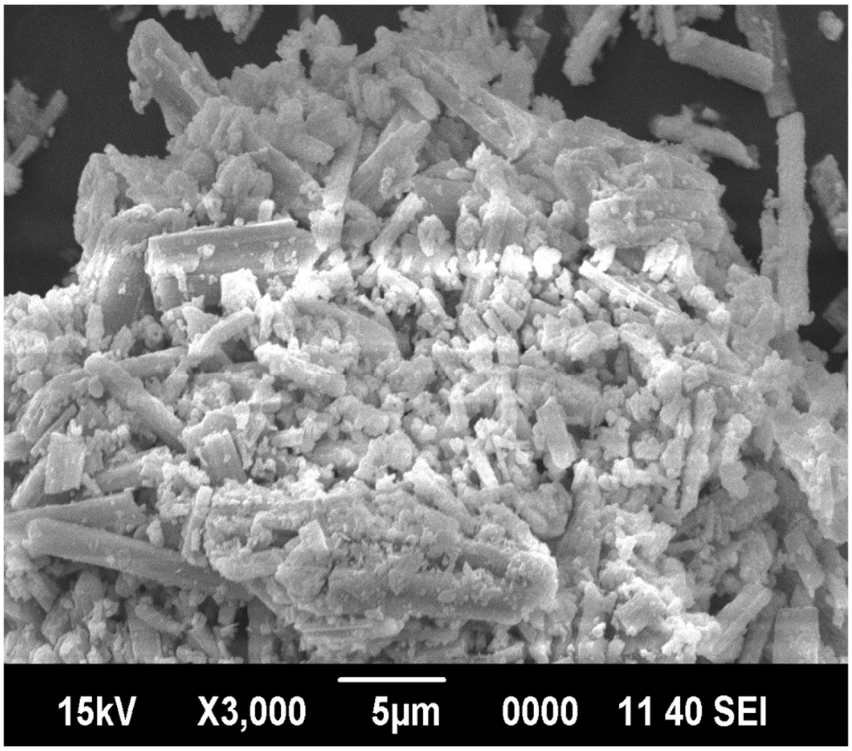

Figure 2: SEM image of as synthesized SnO_2

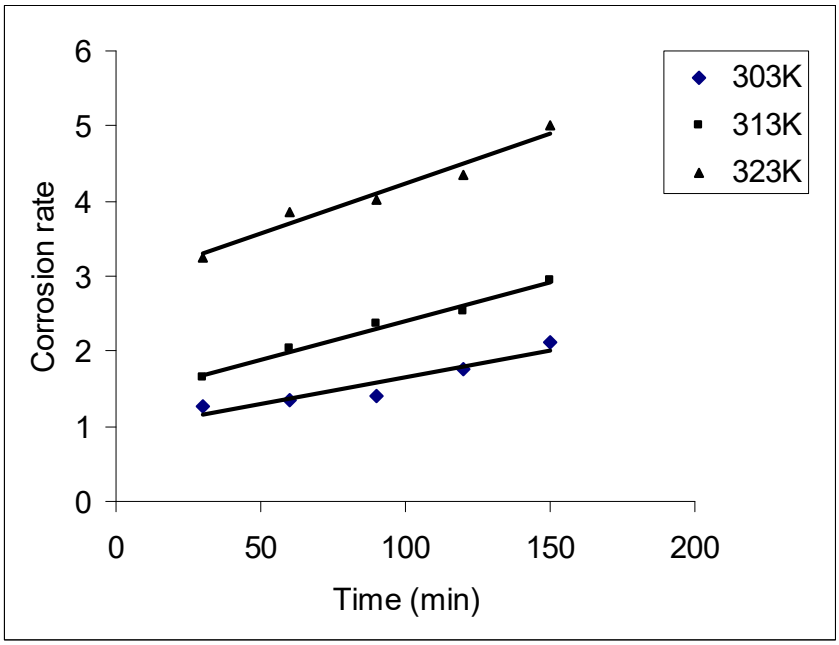

Figure 3: Effect of time on rate of corrosion of aluminium in 5% HCl at various temperatures

Effect of inhibitors

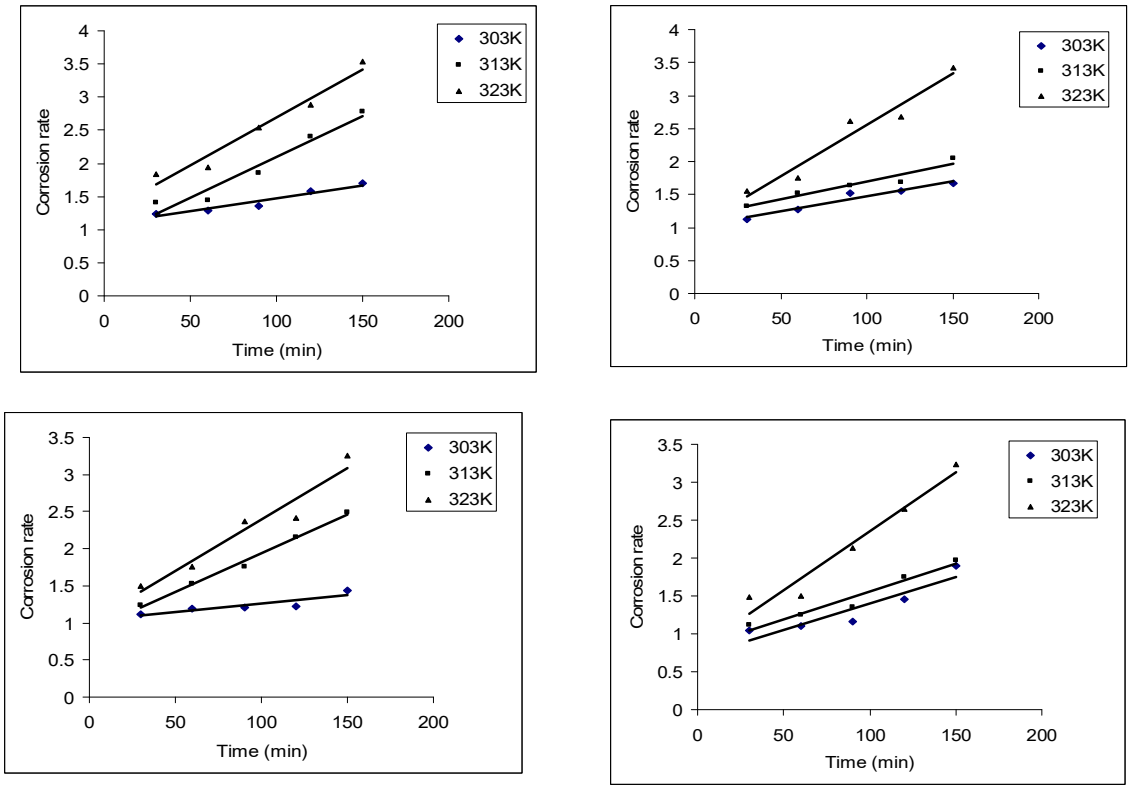

Figure 4: Effect of time on rate of corrosion of aluminium in 5% HCl with 0.01, 0.02, 0.03, 0.04 gpl inhibitor at various temperatures

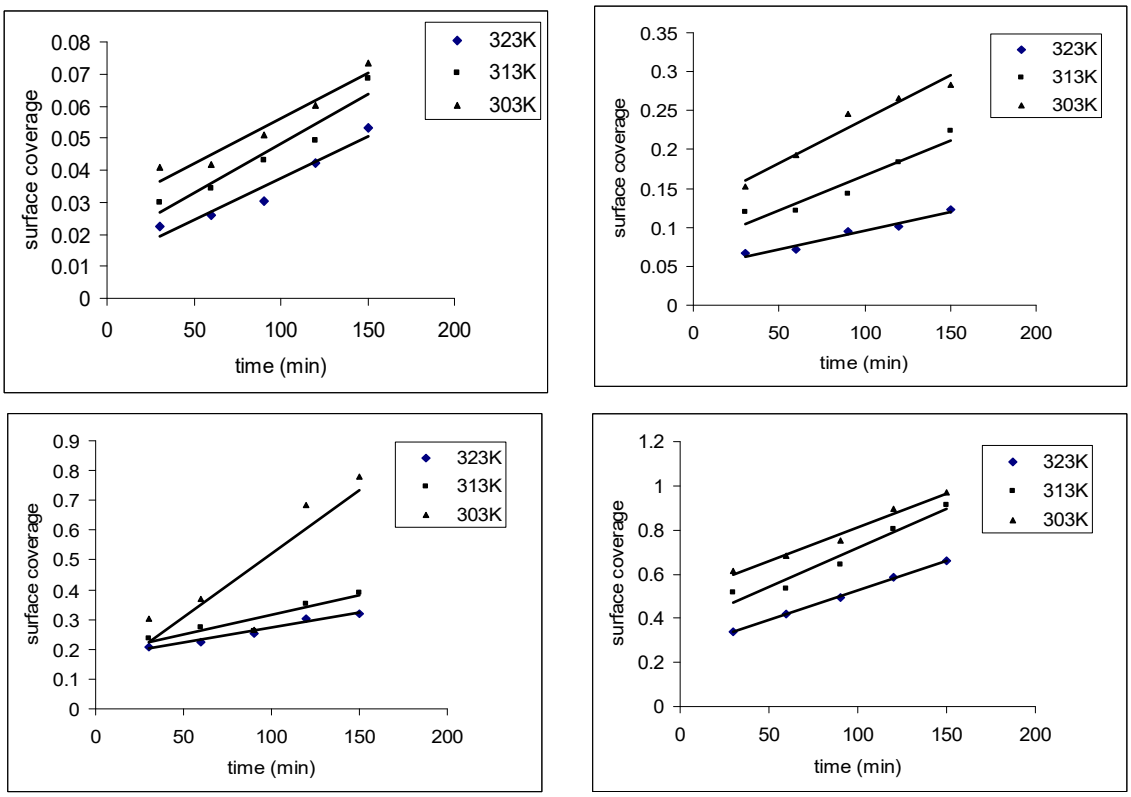

Figure 5: Effect of time on surface coverage of 0.01, 0.02, 0.03, 0.04 gpl inhibitor on aluminium at various temperatures

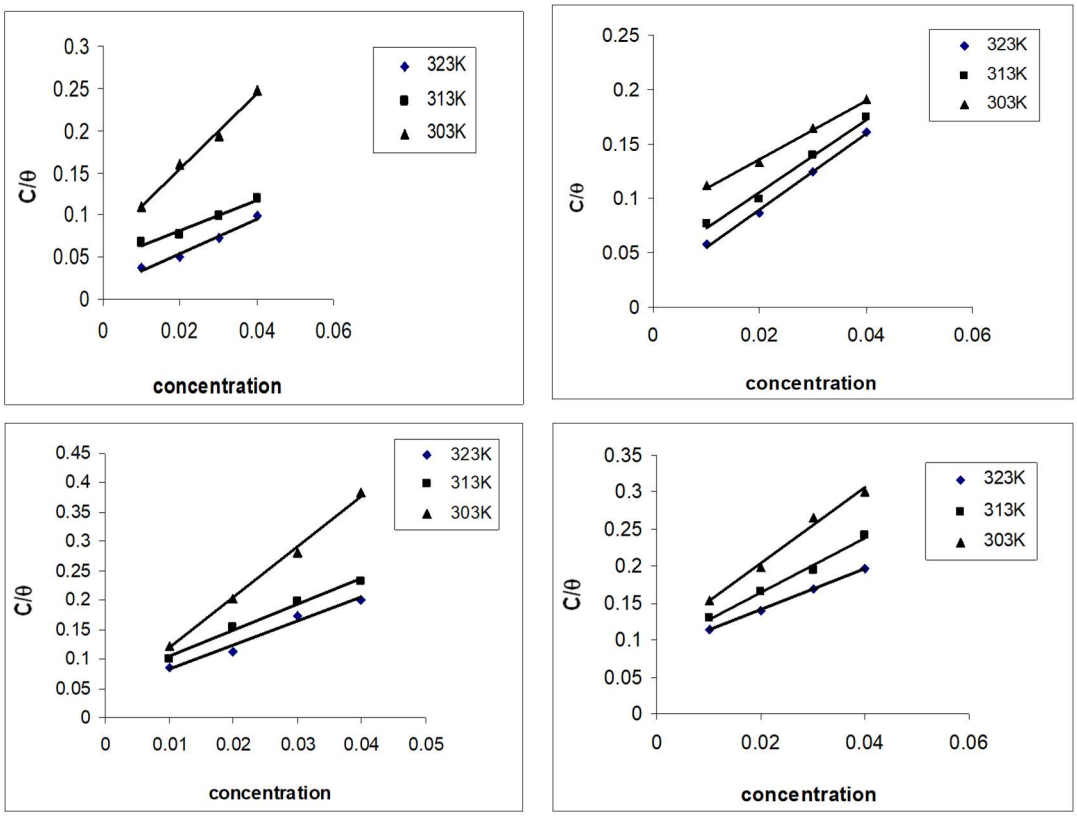

Figure 6: Langmuir plots for corrosion inhibition of aluminium for 30, 60, 90, 120 minutes at various temperatures

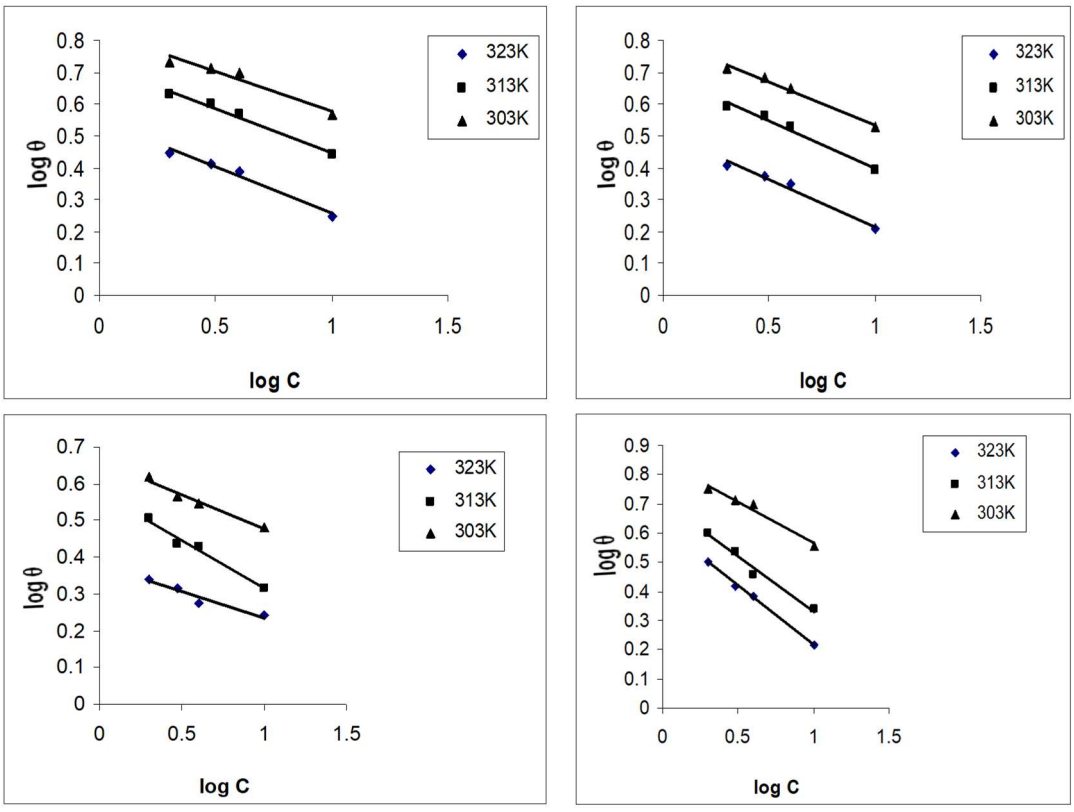

Figure 7: Freundlich plots for corrosion inhibition of aluminium for 30, 60, 90, 120 minutes at various temperatures

Table 1: Electrochemical Parameters obtained from Tafel polarization and electrochemical impedance spectroscopy studies

	Tafel parameters			Impedance parameters		
	E_{corr} (V)	I_{corr} (A)	R_{corr} (MPY)	R_s (Ohm)	C (F)	R_p Ωcm^{-1}
0.01	-0.763	1.267e+006	5.435e+011	1.83e-005	1.372e-005	318.5
0.02	-0.754	1.243e+006	5.333e+011	2.044e-005	1.329e-005	370.1
0.03	-0.745	8.881e+005	3.809e+011	5.014e-005	1.205e-005	764.8
0.04	-0.721	4.386e+005	1.881e+011	6.401e-010	9.641e-006	917.9
0.05	-0.724	7.302e+005	3.132e+011	8.41e-006	1.225e-005	869.1
bare	-0.770	1.483e+006	6.359e+011	4.05e-005	1.523e-005	116.8

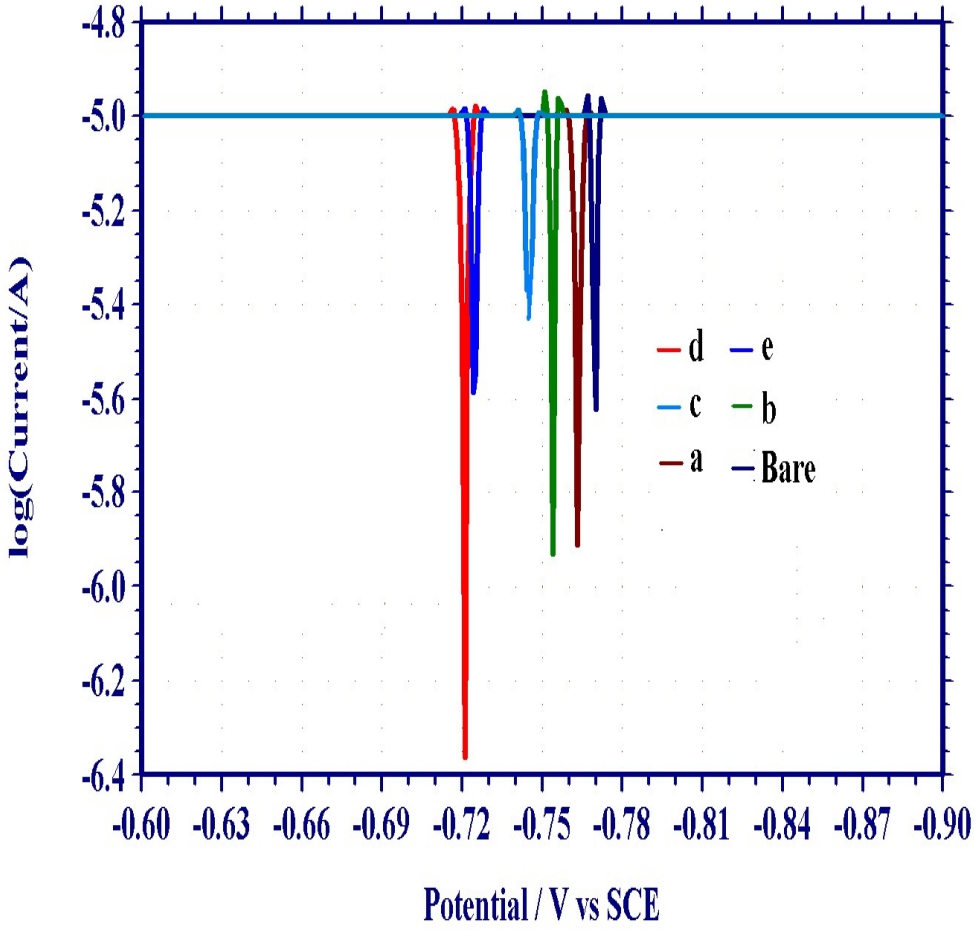

Figure 8: Tafel polarization curves for corrosion of aluminium in 5% HCl without (a) and with (b) 0.01gpl SnO_2 (c) 0.02gpl SnO_2 (d) 0.03gpl SnO_2 (e) 0.04 gpl SnO_2

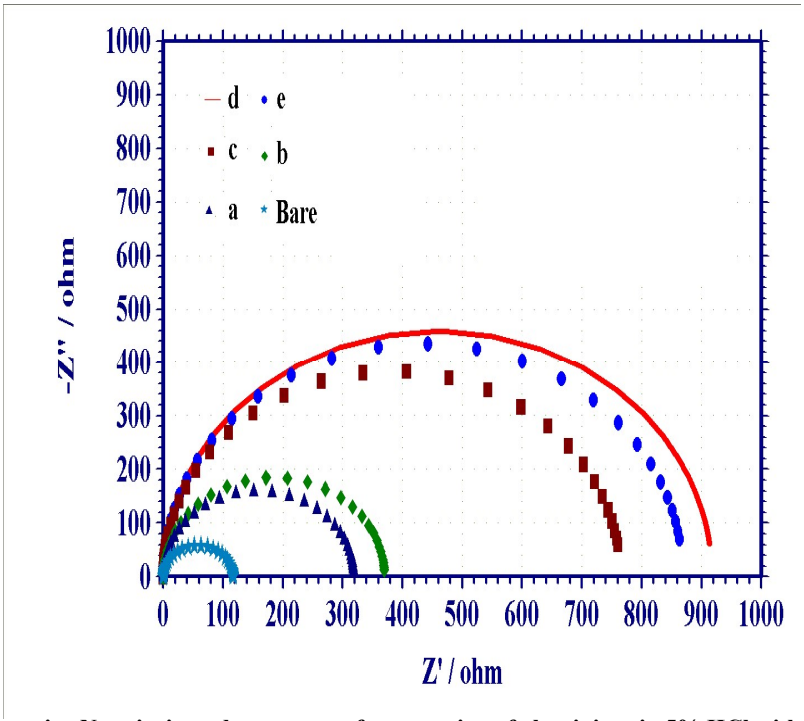

Figure 9: Comparative Nyquist impedance curves for corrosion of aluminium in 5% HCl without (a) and with (b) 0.01gpl SnO_2 (c) 0.02gpl SnO_2 (d) 0.03gpl SnO_2 (e) 0.04 gpl SnO_2

CONCLUSION

Extremely fine stannous oxide nanorods were synthesized by novel simple chemical method. The process parameters such as concentration of $SnCl_2$ phosphoric acid and HCl, stirring time, process temperature and other conditions were optimized to get ultra-fine nanorods. The nanostructure, surface morphology and size of the nanorods were studied by SEM and XRD. The corrosion resistance behaviour of the SnO_2 nanorods has been studied by using it as inhibitor for corrosion of Aluminium in 5% HCl by weight loss, Tafel polarization and electrochemical impedance spectroscopy methods. From the SEM and XRD analyses it can be concluded that, the synthesized SnO_2 is rod shaped with average crystallite size ranging from 4 to 173 nm. From corrosion studies it can be concluded that, the SnO_2 nanorods can be used as a potential inhibitor for corrosion of aluminium in 5% HCl if the concentration is > 0.04 gpl.

REFERENCES

[1] E.E. Stansbury, R.A. Buchanan, Fundamentals of Electrochemical Corrosion, ASM international, 2000.

[2] L.M. Baena, M. Gómez, J.A. Calderón, Aggressiveness of a 20% bioethanole80% gasoline mixture on autoparts: I behavior of metallic materials and evaluation of their

electrochemical properties, Fuel 95 (2012) 320-328.

[3] M.J. Anjum, J. Zhao, V. Zahedi Asl, G. Yasin, W. Wang, S. Wei, Z. Zhao, W. Qamar Khan, In-situ intercalation of 8-hydroxyquinoline in Mg-Al LDH coating to improve the corrosion resistance of AZ31, Corros. Sci. (2019),

[4] G.W. Walter, A critical review of the protection of metals by paints, Corros. Sci. 26 (1986) 27-38.

[5] P.A. Sørensen, S. Kiil, K. Dam-Johansen, C.E. Weinell, Anticorrosive coatings: a review, J. Coat. Technol. Res. 6 (2009) 135-176.

[6] D.G. Shchukin, M. Zheludkevich, K. Yasakau, S. Lamaka, M.G.S. Ferreira, H. Möhwald, Layer-by-layer assembled nanocontainers for self-healing corrosion protection, Adv. Mater. 18 (2006) 1672-1678.

[7] H. Wang, R. Akid, A room temperature cured solegel anticorrosion pre-treatment for Al 2024-T3 alloys, Corros. Sci. 49 (2007) 4491e4503.

[8] A.S.H. Makhlouf, 3etechniques for synthesizing and applying smart coatings for material protection, in: A.S.H. Makhlouf (Ed.), Handbook of Smart Coatings for Materials Protection, Woodhead Publishing, 2014, pp. 56-74.

[9] H. Choi, K.Y. Kim, J.M. Park, Encapsulation of aliphatic amines into nanoparticles for self-healing corrosion protection of steel sheets, Prog. Org. Coat. 76 (2013) 1316-1324.

[10] D. Raps, T. Hack, J. Wehr, M.L. Zheludkevich, A.C. Bastos, M.G.S. Ferreira, O. Nuyken, Electrochemical study of inhibitor-containing organic-inorganic hybrid coatings on AA2024, Corros. Sci. 51 (2009) 1012-1021.

[11] G. Blustein, A.R. Di Sarli, J.A. Jaén, R. Romagnoli, B. Del Amo, Study of iron benzoate as a novel steel corrosion inhibitor pigment for protective paint films, Corros. Sci. 49 (2007) 4202-4231.

[12] J. Sinko, Challenges of chromate inhibitor pigments replacement in organic coatings, Prog. Org. Coat. 42 (2001) 267-282.

[13] N.C. Rosero-Navarro, S.A. Pellice, A. Durán, M. Aparicio, Effects of Ce-containing solegel coatings reinforced with SiO2 nanoparticles on the protection of AA2024, Corros. Sci. 50 (2008) 1283-1291.

[14] G. Decher, J.D. Hong, J. Schmitt, Buildup of ultrathin multilayer films by a self-assembly process: III. Consecutively alternating adsorption of anionic and cationic polyelectrolytes on charged surfaces, Thin Solid Films 210-211 (1992) 831-835.

[15] M.L. Zheludkevich, D.G. Shchukin, K.A. Yasakau, H. Möhwald, M.G.S. Ferreira, Anticorrosion coatings with self-healing effect based on nanocontainers impregnated with corrosion inhibitor, Chem. Mater. 19 (2007) 402-411.

[16] J. Khodabakhshi, H. Mahdavi, F. Najafi, Investigation of viscoelastic and active corrosion protection properties of inhibitor modified silica nanoparticles/epoxy nanocomposite coatings on carbon steel, Corros. Sci. (2018),

[17] Q. Yuan, H.-H. Ge, J.-Y. Sha, L.-T. Wang, C. Wan, F. Wang, K. Wu, X.-J. Meng, Y.-Z. Zhao, Influence of Al2O3 nanoparticles on the corrosion behavior of brass in simulated cooling water, J. Alloy. Comp. 764 (2018) 512-522.

[18] W. Liu, Q. Xu, J. Han, X. Chen, Y. Min, Corros. Sci. 110 (2016) 105–113.

[19] E.A. Matter, S. Kozhukharov, M. Machkova, V. Kozhukharov, Corros. Sci. 62 (2012) 22–33.

[20] X. Li, Q. Zhang, Z. Guo, T. Shi, J. Yu, M. Tang, X. Huang, Appl. Surf. Sci. 342 (2015) 76–83.

[21] A.S. Hamdy, D.P. Butt, J. Mater. Process. Tech. 181 (2007) 76–80.

[22] T.M. Yue, L.J. Yan, C.P. Chan, C.F. Dong, H.C. Man, G.K.H. Pang, Surf. Coat. Tech. 179 (2004) 158–164.